Science of the Total Environment 850 (2022) 157992

Contents lists available at ScienceDirect

Science of the Total Environment

journal homepage: www.elsevier.com/locate/scitotenv

Nitrogen addition and warming rapidly alter microbial community compositions in the mangrove sediment

Changyi Xie [a], Xingyu Ma [a], Yan Zhao [b,c], Tianjiao Dai [a], Weimin Song [b,d], Qi Qi [a], Jianxiang Feng [c,e], Xiaowei Cui [b,c], Jian Zhou [b,c], Xiaofang Huang [f], Fei Qi [g], Yufei Zeng [a], Jizhong Zhou [h,i], Guanghui Lin [b,c,*], Yunfeng Yang [a,**]

[a] State Key Joint Laboratory of Environment Simulation and Pollution Control, School of Environment, Tsinghua University, Beijing 100084, China
[b] Ministry of Education Key Laboratory for Earth System Modeling, Department of Earth System Science, Tsinghua University, Beijing 100084, China
[c] Key Laboratory of Stable Isotope and Gulf Ecology, Institute of Ocean Engineering, Tsinghua Shenzhen International Graduate School, Shenzhen 518055, China
[d] The Yellow River Delta Ecology Research Station of Coastal Wetland, Yantai Institute of Coastal Zone Research, Chinese Academy of Sciences, Yantai 264003, China
[e] School of Life Sciences, Sun Yat-Sen University, Guangzhou 510275, China
[f] CAS Key Laboratory of Tropical Marine Bio-Resources and Ecology, Guangdong Provincial Key Laboratory of Applied Marine Biology, South China Sea Institute of Oceanology, Chinese Academy of Sciences, Guangzhou 510301, China
[g] College of Biological Science and Engineering, Fuzhou University, Fuzhou 350108, China
[h] Institute for Environmental Genomics and Department of Microbiology and Plant Biology, University of Oklahoma, Norman, OK 73019, USA
[i] Earth Sciences Division, Lawrence Berkeley National Laboratory, Berkeley, CA 94720, USA

HIGHLIGHTS

- It is one of the first laboratory-based studies to simulate the mangrove ecosystem.
- N had stronger effects on bacterial, fungal, and functional community compositions than W.
- N increased bacterial richness, evenness, and phylogenetic diversity, owing to strong stochastic processes.
- Changes in nitrogen cycling genes explained higher N_2O efflux induced by N.
- W gave rise to higher carbon degradation potentials.

GRAPHICAL ABSTRACT

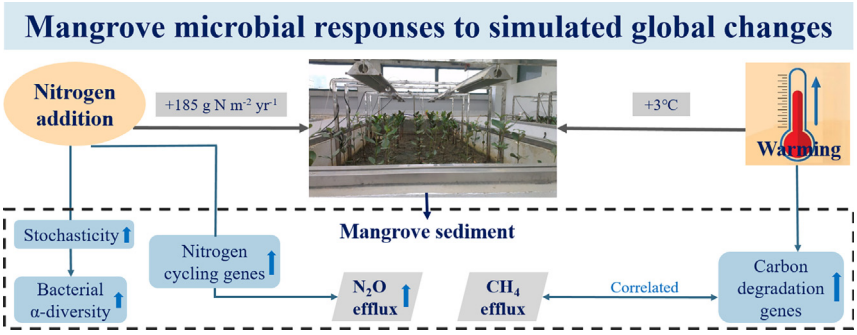

ARTICLE INFO

Editor: Fang Wang

Keywords:
Bacterial and fungal community
Functional community
Nitrogen addition
Climate warming
Stochasicity

ABSTRACT

The mangrove ecosystem is an important CO_2 sink with an extraordinarily high primary productivity. However, it is vulnerable to the impact of climate warming and eutrophication. While there has been extensive research on plant growth and greenhouse gas emission in mangrove ecosystems, microbial communities, the primary biogeochemical cycling drivers, are much less understood. Here, we examined whether short-term experimental treatments: (1) eutrophication with a supplement of 185 g N m^{-2}·$year^{-1}$ (N), (2) 3°C warming (W), and (3) the dual treatment of N and W (NW) were sufficient to alter microbial communities in the sediment. After 4 months of experiments, most environmental factors remained unchanged. However, N had significant, strong effects on bacterial, fungal, and functional community compositions, while the effects of W on microbial communities were weaker. N increased bacterial richness, phylogenetic diversity, and evenness, owing to stronger stochastic processes induced by eutrophication. There were no interactive effects of N and W on bacterial, fungal, and functional community compositions, suggesting that joint effects of N and W were additive. Concomitant with higher N_2O efflux induced by N, the relative abundances of most bacterial nitrogen cycling genes were increased or remained changed by N. In contrast, N decreased or did

* Correspondence to: G. Lin, Ministry of Education Key Laboratory for Earth System Modeling, Department of Earth System Science, Tsinghua University, Beijing 100084, China.
** Corresponding author.
E-mail addresses: lingh@tsinghua.edu.cn lin.guanghui@sz.tsinghua.edu.cn (G. Lin), yangyf@tsinghua.edu.cn (Y. Yang).

http://dx.doi.org/10.1016/j.scitotenv.2022.157992
Received 19 April 2022; Received in revised form 10 July 2022; Accepted 8 August 2022
Available online 13 August 2022

not change those of most bacterial carbon degradation genes, while W increased or did not change the relative abundances of most of bacterial and fungal carbon degradation genes, implying higher carbon degradation potentials. As the most abundant inorganic nitrogenous species in mangrove sediment, ammonium was a key factor in shaping microbial functional communities. Collectively, our findings showed that microbial community compositions in the mangrove sediment were highly sensitive to short-term N and W treatments, giving rise to ecological consequences such as higher N_2O efflux.

1. Introduction

Residing in the intertidal swamps of tropical and subtropical regions, mangrove ecosystems support a great variety and abundance of wildlife. Although it occupies <0.1% of the global area (Spalding and Leal, 2021), it contributes 41 Tg C $year^{-1}$ in C accumulation, equivalent to approximately 13% of the land CO_2 sink and 15% of ocean CO_2 sink (Friedlingstein et al., 2022; Wang et al., 2021). However, eutrophication and climate warming are threatening mangrove ecosystems worldwide. Although nutrient enrichment is beneficial for mangrove growth, it can adversely affect the mangrove ecosystem via elevating sensitivity to hypersalinity (Sarker et al., 2019), harmful algal blooms (HABs) (Thakur et al., 2021), anoxia (Cao et al., 2016), and phosphorus limitation (Luo et al., 2017). Meanwhile, global warming with declines in humidity and rainfall has reduced productivity in many mangrove forests by accentuating midday depressions in photosynthesis (Reef et al., 2010) and causing a widespread die-off of mangroves along arid coasts (Lovelock et al., 2017). Largely driven by anthropogenic activities, mangroves had an estimated net decrease of 3700 km^2 from 1999 to 2019 (Murray Nicholas et al., 2022).

Bacteria and fungi in the mangrove sediment constitute 91% of the total microbial biomass in mangrove ecosystems, which are essential regulators of biogeochemical cycling (Alongi, 1988). Low levels of nitrogen input sequestrate carbon in the sediment but high levels of nitrogen input cause carbon loss, with substantial changes in the bacterial and fungal abundance (Luo et al., 2017). Nitrogen addition also changed bacterial community composition, accompanied by changes in the enzymatic activities associated with elements cycling (Craig et al., 2021). Notably, nitrifying microorganisms can be identified from high-throughput sequencing data since they are comprised of only several genera (Koops and Pommerening-Röser, 2001). Alternatively, they can be identified by biomarker genes of the nitrification process (i.e., *amo*A gene encoding ammonia monooxygenase). In contrast, biomarker genes of *nar*G encoding nitrate reductase, *nir*K encoding nitrite reductase, *nir*S encoding nitrite reductase, *nor*B encoding nitric oxide reductase, and *nos*Z encoding nitrous oxide reductase are commonly used to identify denitrifying microorganisms comprised of a wide range of bacteria (Gruber and Galloway, 2008). Denitrification rates by microorganisms are typically high in mangrove ecosystems because of anaerobic conditions, which deplete the nitrate (NO_3^--N) and nitrite (NO_2^--N) pools. As a result, ammonium (NH_4^+-N) is the most abundant inorganic nitrogenous species in the mangrove sediment (Reef et al., 2010).

Warming stimulates denitrification in mangrove ecosystems (Bai et al., 2013; Shiau et al., 2016), probably owing to the propagation of denitrifiers (Braker et al., 2010). Likewise, warming stimulates nitrification and soil respiration, yielding more substrate and consuming more O_2 favorable for denitrification (Bai et al., 2013). Warming also increases soil organic matter mineralization in mangrove ecosystems (Lewis et al., 2014), with the temperature being the most important factor in shaping the comammox and sulfur cycling microbial communities (Li et al., 2021; Liu et al., 2020). However, there has not been a study of microbial community compositions and functions in the mangrove sediment under both nitrogen addition and warming, thus it remains unknown whether and how nitrogen addition and warming interactively affect microbial communities. Furthermore, ecological processes, such as stochastic or deterministic processes underlying microbial community assembly, have not been examined.

Here, we carried out a study to examine microbial communities in the mangrove sediment subjected to the experimental simulation of 3°C warming (W) and eutrophication with 185 $g{\cdot}m^{-2}{\cdot}year^{-1}$ nitrogen addition (N), which represents the highest N level in mangrove water affected by aquaculture wastewater discharge in southern China (Wu et al., 2014). We used high-throughput amplicon sequencing technology to target bacterial and fungal biomarker genes. We also used a microarray named GeoChip to target a variety of functional genes. Given that microbial communities are generally sensitive to external disturbances and mangrove ecosystem is a "hotspot" for climate change studies (Lovelock et al., 2017; Ma et al., 2019; Reef et al., 2010), we hypothesize that N and W treatments could alter microbial communities in the mangrove sediment, leading to changes in nutrient cycling.

2. Materials and methods

2.1. Experimental design

It was a laboratory-based experiment with a fully factorial design to set up a mangrove ecosystem. There were 16 plots, which were randomly divided into 4 groups with 4 replicates (i.e., the groups of control (CK), N, W, and NW). Specifically, the indoor tide system was set up in a roof greenhouse in Shenzhen, Guangdong Province, China (22°59′ N, 113°97′ E). It consisted of 16 cement tanks (2.40 m × 1.10 m × 0.50 m) as experimental tanks and two additional cement tanks (7.50 m × 1.00 m × 0.70 m) as seawater reservoirs (Fig. S1). One reservoir was connected to tanks with nitrogen addition. The other was connected to tanks without the N treatment by pipelines of seawater input (used during tide flooding periods) and output (used in tide falling periods). Seawater was generated by dissolving natural sea salt in tap water at a salinity of 14 $g{\cdot}L^{-1}$, representing average salinity in a typical mangrove environment of the Southern China Sea (Chen et al., 2013). Submersible pumps and timers were installed to simulate diurnal tides for all the tanks. Seawater was pumped from the reservoir to each tank, reaching a depth of 5 cm during the high tide period (6 h, from 14:00 to 20:00 at local time). Seawater was drained by gravitational force to the reservoir during the low tide period (18 h). Each tank was conditioned under the tidal regime with one tidal cycle a day for one month before starting the experiment to allow mangrove trees to establish and acclimate in the greenhouse. Tidal water in each reservoir was rotated for about seven days as a water cycle, then drained and replenished by new seawater.

Every tank was filled with mangrove mudflat (20%) from Zhanjiang Mangrove Natural Reserve located in Gaoqiao, Lianjiang, Guangdong Province (21°31′-21°34′ N, 109°44′-109°47′ E) and sugarcane soil (80%). After stones, benthic animals, and plant residues in the soil were removed, a padding mixture of soil was put into each tank at a depth of 30 cm. The saplings of *Avicennia marina* (white mangrove) were collected from the mangrove sapling farm of Leizhou, Guangdong Province, and cultivated in the roof greenhouse in the sand for three months for adaptation before transplanting into the tanks. Saplings with an approximately equal height of 30.0 cm and basal diameter of 6.5 mm were used. In every tank, *A. marina* saplings were planted in five rows and five columns, covering half of each tank. As a result, every sapling covered an area of 0.2 m × 0.2 m.

To establish the W treatment, infrared radiators (Kalglo electronics Inc., Bethlehem, PA, USA) were suspended for 0.8 m above the tank for continuous heating (Fig. S1). A temperature inductive probe in each tube was used to heat air through Temperature Control System (Grant and Pattey, 2008). Air near the canopy top of the warming plot was heated by 3°C, the projected median temperature rise by 2100 relative to 1986–2005 based on the scenario with very high GHG emissions (i.e., RCP8.5,

Representative Concentration Pathway 8.5) (IPCC, 2014). In each non-warming mesocosm, 'dummy' heaters with the same shape and size as the infrared heater was installed for 0.8 m above the tank to simulate the shading effects of the infrared radiator. The N treatment was conducted once a week with 20 mg N L^{-1} NH_4^+-N and 5 mg N L^{-1} NO_3^--N (equal to 185 g N m^{-2}·$year^{-1}$) in seawater, based on an observed N level in mangrove water affected by aquaculture wastewater discharge in southern China (Wu et al., 2014). Both manipulations were initiated on March 15th, 2015. Physicochemical properties and plant properties in the sediment were similar among all tanks at the beginning of the experiment.

2.2. Greenhouse gas efflux and plant biomass measurements

Gas samplings were collected on July 8th, 2015, four months after the experiment began and the third day after changing new seawater to maintain N effects (Jia et al., 2016). Greenhouse gas efflux in each tank was quantified using the standard static (closed) chamber technique. In brief, each chamber covered an area of 0.025 m^2 and had an internal volume of 4.0 L. The chamber was placed in a location without mangrove seeding, above-ground root, and litter. The open end of the chamber was inserted into the sedimental soil about 3–5 cm with the airtight valve open. A thermometer was inserted into the soil at 10 cm away from the chamber to measure soil temperature during gas collection. The deployment time was 30 min before sampling collection at 15–30 min' intervals between 9:00 am and 11:00 am. For each sampling, 5 mL of gas samples were collected by passing a hypodermic needle attached to a 10 mL glass syringe (SGE Analytical Science, Ringwood, VIC, Australia) through the air sampling port (Jia et al., 2016). All samples were stored in gas bags and analyzed within 24 h. The N_2O concentration was determined using a gas chromatograph (Agilent 7890A, Agilent Technologies, Santa Clara, CA, USA) equipped with an electron capture detector and an HP- Plot/column (J&W GC Columns, Agilent Technologies, Santa Clara, CA, USA). The CO_2 and CH_4 concentrations were determined by Agilent Hewlett Packard 7890 GC (Agilent Technologies, Santa Clara, CA, USA) equipped with a thermal conductivity detector and a Poro-Pak-Q column, with N_2 as the carrier gas. The greenhouse gas concentrations were quantified by comparing the peak areas of samples to the standard curves.

Avicennia marina biomass was evaluated by a non-destructive allometric technique on August 13th, 2015 (Snedaker and Snedaker, 1984). We measured stem height (H) and basal diameter (D) (at 1 mm above the soil surface) by using a caliper. The relationships between aboveground biomass (AGB), belowground biomass (BGB) and basal diameter (D), stem height (H) were obtained by harvesting 16 individuals of *Avicennia marina* from every mesocosm randomly. The best-fit equations of *Avicennia marina* for estimating aboveground biomass (AGB), belowground biomass (BGB) were $AGB = 5334.9\ D \times D \times H + 0.0114$ ($R^2 = 0.82$), $BGB = 0.4154\ AGB + 0.0059$ ($R^2 = 0.80$).

2.3. Sampling and analyses of the sediment

On the same day as gas efflux measurement (i.e., July 8th, 2015), two independent sedimental soil cores at a depth of 0–20 cm in each tank were collected using hand-held PVC corers (25 mm diameter), and mixed into one composite sample. Soil water content (%) was determined by calculating the proportion of weight loss after oven drying under 105°C for 48 h. Soil pH and soil salinity were measured using a pH/Sa meter (WP-81, TPS, Brendale, QLD 4500, Australia) by inserting the platinum probe into the soil extracting solution (ratio of water to soil is 1:5). Subsamples for microbial analysis were stored at −80°C. Other sub-samples for geophysical and geochemical analyses were oven-dried and sieved through a 0.5 mm sieve.

Soil total carbon (TC, %) and nitrogen (TN, %) contents were measured by Elemental Analyzer (Flash 2000 EA-HT, Thermo Fisher Scientific, Waltham, MA, USA) with 100 mg freeze-dried and 0.25 mm-sieved soil samples. Soil carbon to nitrogen ratio (TC/TN) was calculated. To measure soil NH_4^+-N, NO_3^--N, and NO_2^--N concentration, 7 g fresh soil mixed with 35 mL KCl (2 M) was shaken for 2 h and centrifuged for 3 min by a centrifuge. We used standard procedures and methods for the determination, including the Sodium salicylate-sodium hypochlorite Method for NH_4^+-N, the UV Spectrophotometer Method for NO_3^--N, and the α-Naphthylamine Method for NO_2^--N. Total phosphorus contents in sieved samples were measured by an ultraviolet spectrophotometer after Kjeldahl digestion. All soil analyses were measured as previously described (Page et al., 1982).

2.4. Soil DNA preparation

Genomic DNA was extracted from 5 g of sediment sample by a freeze-grinding procedure as described previously (Wu et al., 2017). Crude DNA was purified by phenol extraction and low melting agarose gel electrophoresis. DNA quality was determined by absorbance ratios of A260/280 nm and A260/230 nm using a NanoDrop ND-1000 Spectrophotometer (NanoDrop Technologies Inc., Wilmington, DE, USA). DNA quantity was determined by PicoGreen using a FLUOstar Optima plate reader (BMG Labtech, Jena, Germany).

2.5. Illumina MiSeq sequencing and raw data processing

High-throughput sequencing of prokaryotic 16S rRNA gene and fungal nuclear ribosomal internal transcribed spacer (ITS) amplicons were used for microbial taxonomy profiling. The V4 region of the 16S rRNA genes was amplified with the primer pair 515F and 806R (5′-GTGCCAGC MGCCGCGGTAA-3′ and 5′-GGACTACHVGGGTWTCTAAT-3′). The ITS region between fungal 5.8S and 28S rRNA genes was amplified with the primer pair gITS7F and ITS4R (5′-GTGARTCATCGARTCTTTG-3′ and 5′-TCCTCCGCTTATTGATATGC-3′). A sequential round of PCR using primers combining Illumina adapter sequences with barcodes was then performed. The MiSeq 500-cycles kit was used for 2 × 250 bp paired-end sequencing on a MiSeq instrument (Illumina Inc., San Diego, CA, USA).

Raw sequence data were processed on the Galaxy platform with a number of software tools (Zhang et al., 2017). First, the quality of raw sequence data was evaluated with FastQC (bioinformatics.babraham.ac.uk/projects/fastqc/). De-multiplexing was performed to remove PhiX sequences, and sequences were sorted into corresponding samples based on their barcodes, allowing for 1 or 2 mismatches. Quality trimming was performed with Btrim (Kong, 2011). Paired-end reads were merged into full-length sequences with FLASH (Magoč and Salzberg, 2011). Sequences <200 bp or containing ambiguous bases were removed. Chimeric sequences based on predictions by Uchime (Edgar et al., 2011) using the reference database mode were discarded. OTUs were generated with Uclust (Edgar et al., 2011) at the 97% similarity level. Taxonomic annotation of individual OTU was assigned according to representative sequences using RDP's 16S rRNA gene classifier (RDP release 11.4) (Wang et al., 2007).

2.6. GeoChip hybridization and data processing

Experiments with GeoChip 5.0 were carried out as previously described (Ma et al., 2019). Briefly, 0.8 μg of DNA was labeled with Cy-3 dye by random priming and purified with a QIA quick purification kit (Qiagen, Valencia, CA, USA). After drying in a SpeedVac (ThermoSavant, Milford, MA, USA) for 45 min at 45°C, labeled DNA was rehydrated with 27.5 μL of DI water. Subsequently, a 99.4 μL of hybridization solution was added. The mixture was loaded onto the gasket slide and hybridized for 20–22 h at 67°C. GeoChip was scanned with a NimbleGen MS 200 microarray scanner (Roche NimbleGen Inc., Pleasanton, CA, USA) as a Multi-TIFF file. The signal intensity of each spot on the microarray was then quantified with the Agilent Feature Extraction program.

Data normalization and analyses of raw data were performed by a data analysis pipeline (ieg.ou.edu/microarray/) as described previously (Yang et al., 2014). The threshold of signal-to-noise ratio SNR = (signal mean - background intensity)/background standard deviation of GeoChip was determined by thermophile probes serving as negative controls. Genes detected in only one of four biological replicates were

removed. Values of remaining genes were then logarithmically transformed, followed by normalization of the signal intensity of each spot by dividing by total abundance.

2.7. Statistical analyses

Differences in microbial taxonomic and functional compositions were examined by Adonis (Permutational multivariate analysis of variance) based on the Bray-Curtis distance, using the *vegan* package. The α-diversity indices, including richness, Shannon index, Simpson index, and Faith's phylogenetic diversity, were calculated with the *ieggr* package. Pielou's evenness was also calculated with the *ieggr* package. The linear model was used to examine the effects of N, W, and their possible interactions on environmental factors, microbial diversity, relative abundances of microbial taxa, and functional genes using the R statistical functions. The stochasticity ratio was calculated based on taxonomic metrics with Bray-Curtis distance, using the *NST* package. The Mantel test was used to analyze the correlations between microbial communities and environmental factors. We considered $P < 0.050$ to be statistically significant unless otherwise indicated. All statistical analyses were conducted with R software (v. 3.6.1.).

3. Results

3.1. Environmental factors

After 4 months of experimental treatments, most environmental factors remained unchanged by experimental treatments. The only exceptions were that N increased the N_2O efflux rate (Linear model, the effect size $\beta = 3.380$ mmol·m^{-2}·h^{-1}, $P = 0.025$; Table S1) and W increased soil temperature (Linear model, $\beta = 3.125$°C, $P < 0.001$; Table S1) and decreased plant biomass (Linear model, aboveground biomass $\beta = -20.387$ g·m^{-2}, $P = 0.041$; belowground biomass $\beta = -8.469$ g·m^{-2}, $P = 0.041$; Table S1). Although N substantially decreased CH_4 fluxes from 0.303 mmol·m^{-2}·h^{-1} to 0.098 mmol·m^{-2}·h^{-1} while W increased them to 0.860 mmol·m^{-2}·h^{-1}, changes in CH_4 and CO_2 fluxes were not statistically significant ($P > 0.050$; Table S1), owing to large variations among biological replicates. There were no interactive effects of N and W on all environmental factors (Linear model, $P > 0.050$; Table S1), suggesting that N and W independently affected environmental factors, i.e., the effect of NW was the additive effect of N and W.

3.2. The taxonomic compositions of bacterial and fungal communities

We obtained a total number of 213,376 sequences of 16S rRNA gene amplicons from all samples. Proteobacteria was the most abundant phylum, accounting for 57.3% of all sequence reads and almost exclusively belonging to α-Proteobacteria, γ-Proteobacteria, and δ-Proteobacteria (Fig. S2a). Other abundant phyla included Bacteroidetes (6.9%), Acidobacteria (6.0%), Firmicutes (5.6%), Actinobacteria (4.0%), Chloroflexi (3.2%), Planctomycetes (1.7%), Chlorobi (1.6%), and Verrucomicrobia (1.2%).

Four months of N treatment increased bacterial richness, Shannon index, Simpson index, Faith's phylogenetic diversity, and Pielou's evenness (Linear model, $\beta = 0.995$–1.060, $P < 0.050$; Table S2), while the effects of W were not significant (Linear model, $P > 0.050$; Table S2). Consistently, N altered bacterial communities, while W did not (Adonis; Table 1), which was verified by the observation that the dissimilarity between CK and W was smaller than the dissimilarity between CK and N (Fig. S3a). There were no interactive effects of N and W on bacterial α-diversity, Faith's phylogenetic diversity, and community composition (Linear model & Adonis, $P > 0.050$; Table S2 & Table 1).

Among abundant bacterial phyla, Proteobacteria, Acidobacteria, Firmicutes, Actinobacteria, Planctomycetes, Verrucomicrobia, Gemmatimonadetes, WS3, and Armatimonadetes were affected by N, while only Planctomycetes and OD1 were affected by W (Linear model, $|\beta| = 0.000$–0.779, $P < 0.050$; Table S3). At the genus level, N increased the relative abundances of Bradyrhizobium, Gp3, Gp6, Gp7, Conexibacter, Bacillus, Spartobacteria_genera_incertae_sedis, Phenylobacterium, Pseudolabrys, Burkholderia, Gemmata, and Mycobacterium (Linear model, $\beta = 0.074$–1.321, $P < 0.050$; Table S3) but decreased those of Singulisphaera and Ktedonobacter (Linear model, $\beta = -0.063 \sim -0.380$, $P < 0.050$; Table S3). W decreased Gp3, Singulisphaera, and Gemmata ($\beta = -0.362 \sim -0.834$) but increased Mycobacterium ($\beta = 0.157$) in relative abundances (Linear model, $P < 0.050$; Table S3). N drecreased the relative abundance of methanogenic genus Methanosaeta (Linear model, $\beta = -0.783$, $P = 0.044$; Table S4), but increased those of bacterial nitrifying (i.e., Nitrobacter and Nitrosococcus) (Linear model, $\beta = 0.648$–0.685, $P < 0.050$; Table S4) and denitrifying genera (i.e., Bradyrhizobium, Bacillus, Burkholderia, Rhodoplanes, Paenibacillus, and Mesorhizobium) (Linear model, $\beta = 0.088$–1.525, $P < 0.050$; Table S4). In contrast, W did not affect any methanogenic or bacterial nitrifying genus (Linear model, $P > 0.050$; Table S4), but increased the relative abundance of denitrifying genus Thiomicrospira (Linear model, $\beta = 1.246$, $P = 0.045$; Table S4).

We generated 39,840 ITS sequences representing fungal communities, which were composed of Ascomycota (54.1%), Basidiomycota (11.8%), Zygomycota (2.5%), Chytridiomycota (1.3%), Clomeromytota (0.9%), and unclassified OTUs (29.4%) (Fig. S2b). Both N and W altered fungal community composition (Adonis, $P < 0.050$; Table 1), while there were not interactive effects of N and W on fungal community composition (Adonis, $P = 0.189$; Table 1). N did not affect fungal diversities and evenness (Linear model, $P > 0.050$; Table S2), while W decreased Faith's phylogenetic diversity (Linear model, $\beta = -0.005$, $P = 0.015$; Table S2).

Table 1
The taxonomic and functional community compositions between control and treatments based on Adonis.

Microbial community	Treatment	Bacteria		Fungi	
		R^2	*P*	R^2	*P*
Taxonomic	N[a]	0.110	**0.001*****[b]	0.084	**0.007****
	W	0.067	0.245	0.082	**0.019***
	N × W	0.074	0.115	0.070	0.189
Functional	N	0.447	**0.001*****	0.430	**0.001*****
	W	0.075	0.095	0.094	**0.042***
	N × W	0.088	0.070	0.091	0.056

[a] Abbreviations: N, Nitrogen addition; W, Warming; N × W, the interactive effect of N and W.
[b] Significant *P*-values: *, $P < 0.050$; **, $P < 0.010$; ***, $P < 0.001$ based on permutational multivariate analysis of variance.

3.3. Ecological mechanisms underlying bacterial and fungal communities

Stochastic and deterministic processes jointly shape microbial community assembly (Stegen et al., 2012). N increased the relative importance of stochastic processes from 56.2% to 73.9% (Linear model, $P = 0.001$; Table 2) in shaping bacterial communities, but decreased the relative

Table 2
Treatment effects on modified stochasticity ratio (MST) based on linear models.

Treatment effects		Bacteria	Fungi
N[a]	β[b]	**0.177**[c]	**−0.022**
	t	**1.868**	**−0.278**
	P	**0.001**	**0.047**
W	β	−0.123	0.060
	t	−1.297	0.767
	P	0.557	0.528
N × W	β	0.166	−0.191
	t	1.237	−1.727
	P	0.230	0.100

[a] Abbreviations: N, Nitrogen addition; W, Warming; N × W, the interactive effect of N and W.
[b] All estimated effect sizes (β) are based on pairwise MST in groups.
[c] Significant *P*-values ($P < 0.050$) are labeled in bold.

importance of stochastic processes from 72.6% to 70.4% (Linear model, $P = 0.047$; Table 2) in shaping fungal communities. In contrast, W did not alter the relative importance of stochastic processes in shaping bacterial and fungal communities. There were no interactive effects of N and W on the relative importance of stochastic processes.

3.4. The functional composition of microbial communities

A total of 51,756 functional genes were detected by GeoChip. Consistent with observations in taxonomic community compositions, N showed much stronger effect on functional composition (functional composition derived from bacteria: $R^2 = 0.447$, functional composition derived from fungi: $R^2 = 0.430$) than W (functional composition derived from bacteria: $R^2 = 0.075$, functional composition derived from fungi: $R^2 = 0.094$) (Adonis, $P < 0.050$; Table 1). Functional composition derived from bacteria were altered by N, while those derived from fungi were altered by N and W. There were not interactive effects of N and W on functional composition (Adonis, $P > 0.050$; Table 1).

We examined whether there was any linkage between taxonomic and functional α-diversities were correlated for bacteria ($R = 0.778$, $P < 0.001$; Fig. S4a) but not fungi (Fig. S4b). Similarly, taxonomic and functional community compositions were also correlated for bacteria ($R = 0.543$, $P < 0.001$; Fig. S4c) but not fungi (Fig. S4d).

3.4.1. Nitrogen cycling genes

Most known nitrogen cycling genes were derived from bacteria. Concomitant with the observation that N increased the N_2O efflux rate (Table S1), we found that N increased or did not affect the relative abundances of most bacterial nitrogen cycling genes except for *amo*A encoding ammonia monooxygenase converting ammonium into NH_2OH, and *nar*G encoding nitrate reductase and *nas*A encoding assimilatory nitrate reductase converting nitrate into nitrite (Linear model, $P < 0.050$; Fig. 1a). In contrast, there were few changes in bacterial nitrogen cycling genes by W (Fig. 1b). The interactive effects of N and W on bacterial nitrogen cycling genes were viable, with the increase in ammonification gene *gdh* encoding glutamate dehydrogenase, and denitrification genes *nor*B encoding nitric oxide reductase and *nir*K encoding nitrite reductase, but the decrease in nitrification *hao* encoding hydroxyacid oxidase, assimilatory N reduction genes *nir* encoding nitrite reductase and *nar*B encoding nitrate reductase (Fig. 1c).

3.4.2. Carbon degradation genes

N decreased or did not affect the relative abundances of most bacterial carbon degradation genes (Linear model, $P < 0.050$; Fig. 2a). In contrast, N effects on relative abundances of fungal carbon degradation genes were highly viable, with the increase in genes encoding xylanase, α-galactosidase, lactase, cellobiase, phospholipase, chitinase, glyoxal oxidase (*glx*), and phenol oxidase but the decrease in genes encoding pectate lyase

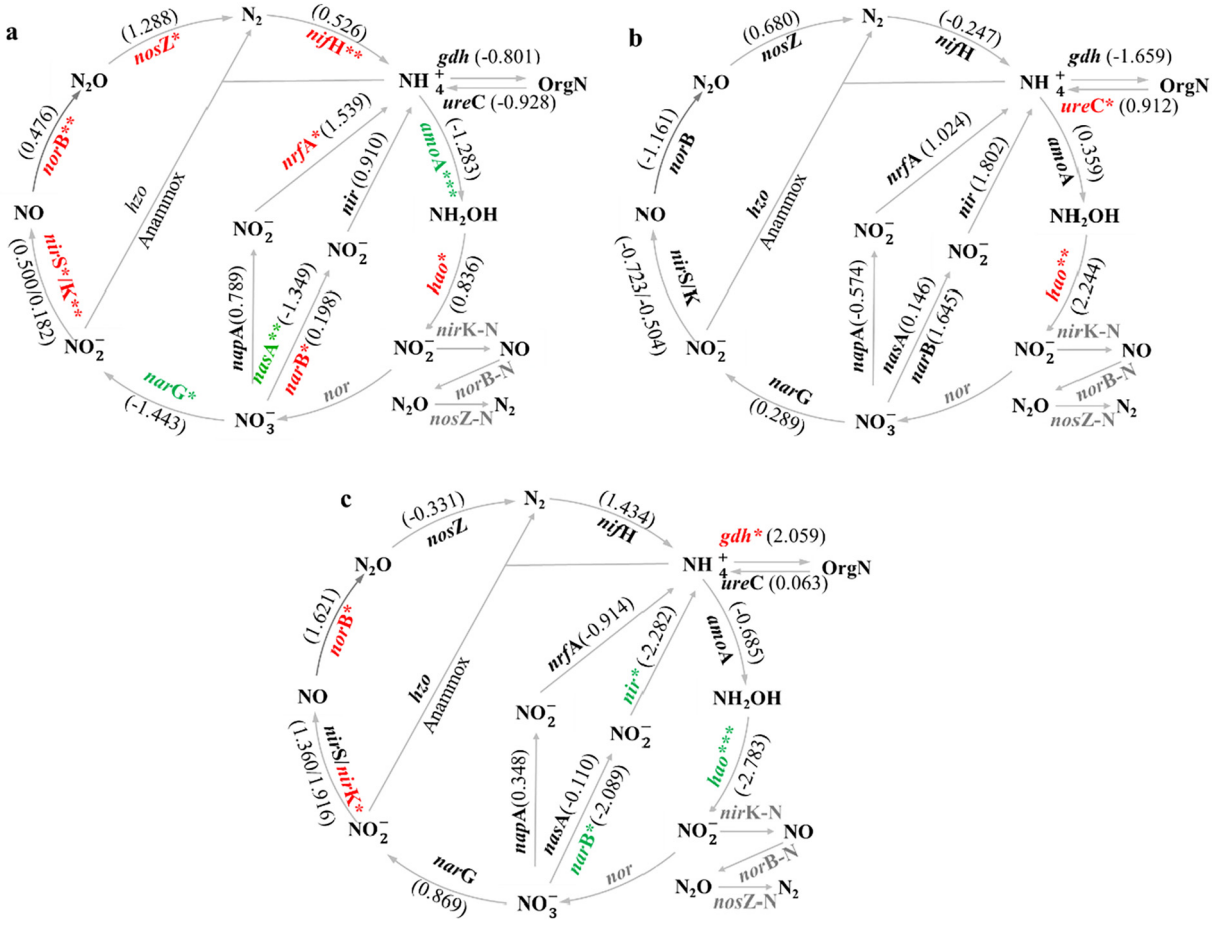

Fig. 1. N and W effects on the relative abundances of bacterial nitrogen cycling genes based on linear models, using GeoChip data. **a**, N: nitrogen addition; **b**, W: warming; **c**, N × W: the interactive effect of N and W. The values in the bracket indicate effect sizes of N, W, and N × W on nitrogen cycling genes. Red color represents a significant increase in the relative abundance, while green color represents a significant decrease in the relative abundance. Black colored genes are not significantly affected, and gray colored genes are not targeted by GeoChip. The statistical significance is based on F tests. Asterisks represent significant *P*-values: *, $P < 0.050$; **, $P < 0.010$; ***, $P < 0.001$.

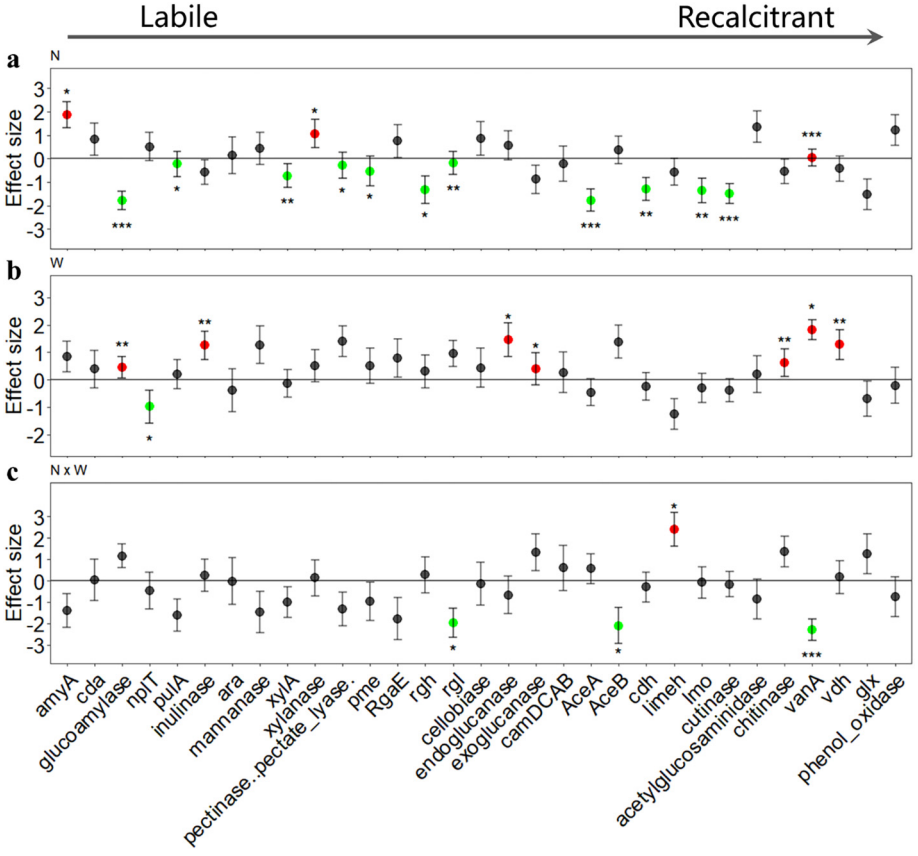

Fig. 2. N and W effects on the relative abundances of bacterial carbon degradation genes based on linear models, using GeoChip data. a, N: nitrogen addition; b, W: warming; c, N × W: the interactive effect of N and W. Red color represents a significant increase in the relative abundance, while green color represents a significant decrease in the relative abundance. Black color represents insignificant changes. The statistical significance is based on F tests. Asterisks represent significant *P*-values: *, $P < 0.050$; **, $P < 0.010$; ***, $P < 0.001$. Error bars represent the standard errors of the estimated effect sizes.

(*pel*), rhamnogalacturonan hydrolase *(rgh)*, tannase, and manganese peroxidase (*mnp)* ($P < 0.050$; Fig. S5a). W increased or did not affect the relative abundances of most bacterial and fungal carbon degradation genes (Fig. 2b & Fig. S5b). The interactive effects of N and W on bacterial carbon degradation genes were viable, with the increase in *limeh* encoding limonene epoxide hydrolase but the decrease in *rgl* encoding rhamnogalacturonan lyase, *Ace*B encoding malate synthase in acetate metabolism, and *van*A encoding vanillate *O*-demethylase (Fig. 2c).

3.4.3. Phosphorus cycling genes

N increased the relative abundance of bacterial *ppk* encoding polyphosphate kinase but decreased that of *ppk*2 encodng polyphosphate kinase 2 (Fig. S6a). W increased the relative abundance of bacterial *ptx*D encodng phosphite oxidoreductase (Fig. S6b).

3.4.4. Sulfur cycling genes

N increased the relative abundances of sulfate reduction gene *Apr*B encoding adenosine 5′-phosphosulfate reductase, sulfite reduction genes *dsr*A encoding dissimilative sulfite reductase and *sir* encoding sulfite reductase, and sulfide oxidation gene *sqr* encoding sulfide:quinone oxidoreductase, but decreased those of bacterial genes encoding dimethylsulfoniopropionate [DMSP] lyase and sulfur oxidase (*sox*Y*)* (Fig. S7a). In contrast, there was no change in bacterial sulfur cycling genes by W (Fig. S7b).

3.5. The linkages between environmental factors and functional microorganisms

Both nitrifying and denitrifying community compositions were significantly or marginally significantly correlated with soil NH_4^+-N concentration, NO_3^--N concentration, and NH_4^+ / NO_3^- ratios, while nitrifying bacteria were correlated with soil temperature, pH, and salinity ($P < 0.100$; Table 3). Since NH_4^+-N stimulates more growth of AOB than AOA (Prosser and Nicol, 2012), we detected a negative correlation between AOA/AOB abundance and NH_4^+-N concentration ($P = 0.005$; Fig. S8), which was also observed in polluted mangrove sediment (Cao et al., 2011). NH_4^+-N concentration appeared to be a key environmental factor in shaping functional community composition, as it was correlated with relative abundances of nitrogen cycling and carbon degradation genes (Table 3).

CH_4 efflux was correlated with methanogens, nitrifying community, denitrifying community, nitrogen cycling, and carbon degradation genes ($P < 0.100$; Table 3). In contrast, CO_2 efflux was not correlated with any functional microorganisms. N_2O efflux was correlated with methanogens and denitrifying community ($P < 0.100$; Table 3).

4. Discussion

Elucidating microbial diversity and community composition in the mangrove sediment is critical for assessing ecosystem stability and functioning. Here, we conducted a short-term experiment to test whether those microbial communities were sensitive to short-term N and W treatments. We found that bacterial, fungal, and functional communities were altered after 4-months treatments (Table 1), showing little interaction between N and W. Those observations support our hypothesis.

4.1. The effects of the N treatment

Our N treatment increased bacterial richness, Shannon index, Simpson index, and Faith's phylogenetic diversity in the mangrove sediment (Table S2). It opposes the common observation that N would decrease the

Table 3
Mantel tests between microbial communities and environmental factors.

Environmental factors	Methanogens				Nitrifying microorganisms				Denitrifying microorganisms				Nitrogen cycling genes		Carbon degradation genes	
	Sequencing data		GeoChip data		Sequencing data		GeoChip data		Sequencing data		GeoChip data					
	r	*P*	r	*P*	r	*P*	r	*P*	r	*P*	r	*P*	r	*P*	r	*P*
Soil T[a] (°C)	−0.135	0.855	0.114	0.150	−0.104	0.825	0.185	**0.059**[b]	−0.143	0.910	0.056	0.296	0.047	0.279	0.045	0.271
Water (%)	−0.031	0.488	0.047	0.336	0.103	0.189	0.012	0.438	−0.127	0.812	0.023	0.392	0.046	0.325	0.077	0.249
pH	0.101	0.243	−0.197	0.958	0.205	**0.090**	−0.198	0.908	−0.116	0.765	−0.163	0.915	−0.147	0.916	−0.141	0.899
Salinity	−0.045	0.507	−0.122	0.797	0.259	**0.083**	−0.149	0.852	−0.170	0.872	−0.085	0.680	−0.100	0.743	−0.092	0.734
TC (%)	0.192	0.121	−0.002	0.498	−0.066	0.659	−0.042	0.560	0.111	0.261	−0.069	0.641	−0.055	0.606	−0.027	0.501
TN (%)	−0.078	0.498	−0.260	0.999	0.184	0.103	−0.310	0.996	−0.203	0.921	−0.229	0.998	−0.224	0.992	−0.219	1.000
TC/TN	−0.084	0.619	−0.077	0.704	0.030	0.358	−0.131	0.806	−0.024	0.556	−0.117	0.805	−0.109	0.786	−0.098	0.753
NO_2^- ($\mu g \cdot g^{-1}$)	−0.104	0.749	−0.103	0.789	0.141	0.125	−0.007	0.489	−0.184	0.970	−0.117	0.841	−0.115	0.829	−0.129	0.899
NH_4^+ ($\mu g \cdot g^{-1}$)	0.092	0.223	0.156	0.124	0.276	**0.057**	0.287	**0.032**	0.139	0.189	0.214	**0.060**	0.189	**0.082**	0.172	**0.094**
NO_3^- ($\mu g \cdot g^{-1}$)	0.285	**0.074**	−0.041	0.570	−0.030	0.529	−0.053	0.627	0.214	**0.083**	−0.033	0.566	−0.015	0.524	−0.021	0.507
NH_4^+/NO_3^-	−0.081	0.612	0.106	0.185	0.289	**0.061**	0.250	**0.065**	0.001	0.432	0.192	**0.080**	0.166	0.118	0.142	0.153
P ($\mu g \cdot g^{-1}$)	0.122	0.171	0.062	0.311	0.001	0.407	0.025	0.433	0.253	0.104	0.023	0.371	0.032	0.339	0.063	0.255
AGB ($g \cdot m^{-2}$)	−0.142	0.799	−0.023	0.549	−0.112	0.787	−0.126	0.786	−0.197	0.947	−0.066	0.679	−0.053	0.621	−0.071	0.690
BGB ($g \cdot m^{-2}$)	−0.142	0.802	−0.023	0.525	−0.112	0.793	−0.126	0.831	−0.197	0.941	−0.066	0.664	−0.053	0.606	−0.071	0.683
N_2O ($mmol \cdot m^{-2} \cdot h^{-1}$)	0.509	**0.060**	0.162	0.115	−0.175	0.918	0.034	0.395	0.311	**0.046**	0.116	0.223	0.109	0.233	0.122	0.205
CH_4 ($mmol \cdot m^{-2} \cdot h^{-1}$)	−0.096	0.613	0.261	**0.046**	0.090	0.234	0.360	**0.015**	−0.052	0.573	0.288	**0.029**	0.276	**0.029**	0.226	**0.063**
CO_2 ($mmol \cdot m^{-2} \cdot h^{-1}$)	0.063	0.296	−0.106	0.825	−0.016	0.464	−0.003	0.490	0.101	0.206	−0.036	0.618	−0.034	0.589	−0.077	0.726

[a] Abbreviations: T, temperature; TC, total carbon; TN, total nitrogen; P, phosphorus; AGB, aboveground biomass; BGB, belowground biomass.
[b] Significant or marginally significant *P*-values ($P < 0.100$) are labeled in bold.

biodiversity of soil microbial communities in forest, grassland, cropland, tundra, desert, and shrub ecosystems, which is frequently caused by soil acidification associated with N (Wang et al., 2018). Accordingly, we observed no change in pH by N (Table S1). In addition, the nitrogen content of manipulated tidal water in this study was high enough to cause seawater eutrophication (Wu et al., 2014), which stimulated fast-growing organisms. Here, we also observed the increase of typical fast-growing bacterial genera such as Bradyrhizobium, Bacillus, and Mycobacterium (Table S3).

Both bacterial and fungal community compositions were altered by N, with the bacterial community showing a more substantial shift ($R^2_{bacteria} = 0.110$ versus $R^2_{fungi} = 0.084$, Table 1). Although we could not exclude the possibility that the difference arose from technical issues such as the choices of primers or PCR conditions, the fungal community composition was likely less sensitive to higher nutrient availability than the bacterial community (Koyama et al., 2014) since the bacterial energy channel is a fast cycle with high turnovers of labile carbon and high mineralization rates, while the fungal-based food web has slower turnover due to more recalcitrant carbon and SOM-associated nutrients (Schröter et al., 2003).

N treatment in terrestrial ecosystems might stimulate nitrogen mineralization rate and N_2O emissions to the atmosphere (Jia et al., 2016; Muñoz-Hincapié et al., 2002; Reis et al., 2017), which was verified by higher N_2O efflux under N addition (Table S1). The increase of N_2O efflux was concomitant with higher relative abundances in many nitrogen cycling genes (Table S1 & Fig. 1a), suggesting that there was higher functional capacity in driving nitrogen cycling. N increased the relative abundance of dissimilatory nitrate reduction gene *nrf*A encoding nitrite reductase (Fig. 1a), known to conserve nitrogen in mangrove sediment (Cao et al., 2016). N also increased the relative abundance of nitrogen fixation gene *nif*H encoding nitrogenase that converts atmospheric nitrogen to NH_4^+-N (Fig. 1a). It aligned with the remarkably increased nitrogen fixation bacteria Bradyrhizobium by N ($\beta = 0.937$, $P = 0.002$; Table S3).

Anaerobic sulfate reduction is an important microbial metabolic pathway to remove electrons and degrade organic matter in the mangrove sediment (Kristensen et al., 2008). It is of interest to find that the functional potential of sulfate reduction was increased by N (Fig. 1a & Fig. S7a), which may be linked to dissimilatory nitrogen reduction because higher sulfate reduction may favor dissimilatory nitrogen reduction over denitrification (Bernard et al., 2015; Brunet and Garcia-Gil, 1996). The reasons are (1) sulfide derived from sulfate reduction can inhibit denitrification and (2) dissimilatory nitrogen reduction yielded higher free energy than denitrification (Aelion and Warttinger, 2010; Thauer et al., 1977). Also, similar to an observation elsewhere (Enebe and Babalola, 2021), N increased relative abundance of *ppk* associated with the synthesis of polyphosphate (Fig. S6), which is important for energy reserves, gene expression, and signaling transduction (Rao et al., 2009; Toso et al., 2011).

4.2. The effects of the W treatment

In this study, 4-months W significantly altered taxonomic and functional compositions of fungal communities (Table 1). Similar results were observed after 1.5-years warming in Arctic permafrost soil, which is well known to be vulnerable to warming (Xue et al., 2016). In contrast, a 4-years W treatment did not affect microbial functional composition, diversities and abundances in the subtropical forest soils, suggesting that four years were not long enough to evoke a response from microbial functional genes (Zhang et al., 2022). Therefore, mangrove ecosystems could be one of the "hotspots" vulnerable to the impact of climate changes. However, bear in mind a caveat that many current studies, including this one, are "snapshots" of microbial communities of a single time point. Changes in microbial communities by external disturbance were likely transient. For example, anammox microbial communities were transiently shifted under elevated salinity but could adapt to the disturbance over time, gradually returning to the original state (Ya et al., 2021). Therefore, longitudinal analyses will be valuable in examining the response of microbial communities in mangrove sediment to external disturbance. However, it has been rare at the functional gene level, partly owing to the high cost of metagenomics or GeoChip tools.

W affected a number of microbial functional groups important for carbon decomposition (Fig. 2b), consistent with metagenomics-based studies that the microorganisms play crucial roles in regulating soil carbon dynamics through shifting microbial communities and stimulating carbon degradation genes (Luo et al., 2014; Zhou et al., 2011). A previous study also found that raising the temperature from 23°C to 27°C in microcosms enhanced potentially mineralizable carbon by 40% (Lewis et al., 2014). The mineralization of sediment carbon could be rapid in the south coastline of China, with a faster rate in summer than in autumn and winter (Alongi et al., 2005). Since these functional genes are related to aerobic carbon degradation, their higher abundance could potentially enhance carbon decomposition and contribute to positive climate feedback, resulting in higher soil respiration in many terrestrial ecosystems (Lei et al., 2021; Xue et al., 2016).

4.3. Ammonium as a key environmental factor influencing functional communities

NH_4^+-N is the most abundant dissolved inorganic nitrogenous species in the mangrove sediment (Reef et al., 2010), it is thus unsurprising that NH_4^+-

N concentration was important in structuring nitrifying, denitrifying, and overall nitrogen cycling communities (Table 3). Similarly, NH_4^+-N concentration was shown to affect ammonia oxidizers in mangrove ecosystems (Liu et al., 2020). In addition, the importance of soil temperature for nitrifying communities (Table 3) has been demonstrated by both meta-analysis and mangrove ecosystem studies (Bai et al., 2013; Liu et al., 2020). In general, our results agree with previous observations that total nitrogen (TN), total carbon (TC), pH, temperature, and salinity were influential for microbial community composition in the mangrove sediment (Craig et al., 2021; Liu et al., 2020; Luo et al., 2017).

4.4. The linkages between greenhouse gas efflux and functional communities

N_2O is a potent greenhouse gas produced as an intermediate product of both nitrification and denitrification (Gruber and Galloway, 2008; Koops and Pommerening-Röser, 2001). N_2O efflux was correlated with the denitrifying community but not the nitrifying community (Table 3), implying that denitrification could be more influential in producing N_2O. This is consistent with previous observations in a mangrove estuary and a marsh landscape that denitrification is responsible for large rates of N_2O emission (Gao et al., 2019; Yang and Silver, 2016), which could be attributed to high soil moisture in mangrove forests (>20%, Table S1). The denitrifying community was also correlated with CH_4 efflux, well known to be strictly controlled by anaerobic conditions (Table 3).

Sedimental CH_4 exchange is affected by pneumatophore number and the redox potential of sediment water at depth (Livesley and Andrusiak, 2012). Since higher sediment temperature was the most significant factor contributing to CH_4 emission (Allen et al., 2007), one might expect that W increases the CH_4 efflux. However, the CH_4 efflux varied from 0.098 to 0.860 $mmol \cdot m^{-2} \cdot h^{-1}$ in our experiment, which was unchanged by W or N (Table S1). Relative abundances of methanogenic taxa were also unchanged by W or N (Table S4), suggesting that the mangrove sediment in this experiment was a small CH_4 source and the CH_4 efflux was irresponsive to the short-term W or N treatment.

We did not find correlations between carbon degradation genes and CO_2 efflux (Table 3), possibly because most carbon mineralized in the subsurface sediment seeps out of the pool via water. The extensive sediment beneath the mangrove is a large respiratory reservoir, with tidal advection and groundwater flow transporting ~70% of total soil respiration (86 Tg C $year^{-1}$) to adjacent waters in the form of dissolved inorganic carbon (Alongi, 2014; Alongi et al., 2012). As a result, in-situ measurements of CO_2 efflux may be under-estimated if CO_2 efflux leaching to adjacent waters is not accounted for.

5. Conclusions

To the best of our knowledge, this is among the first laboratory-based studies to analyze microbial communities in mangrove sediments subjected to simulated N and W. Our results suggested that short-term N and W rapidly altered microbial communities, linking to higher N_2O efflux under N. As a crucial carbon sink in the sea-land interface, the stability of old carbon in the mangrove sediment may be substantially altered by W. These findings will improve our understanding of microbial responses to N and W in mangrove ecosystems since estimating changes in future carbon sinks in mangrove ecosystems hinges on our ability to understand the biogeochemical consequences of N, W, and the interactions between them.

CRediT authorship contribution statement

Changyi Xie: Formal analysis, Writing – original draft. **Xingyu Ma:** Formal analysis, Writing – review & editing. **Yan Zhao:** Investigation. **Tianjiao Dai:** Formal analysis, Writing – original draft. **Weimin Song:** Investigation. **Qi Qi:** Formal analysis. **Jianxiang Feng:** Investigation. **Xiaowei Cui:** Investigation. **Jian Zhou:** Investigation. **Xiaofang Huang:** Investigation. **Fei Qi:** Investigation. **Yufei Zeng:** Formal analysis. **Jizhong Zhou:** Writing – review & editing. **Guanghui Lin:** Funding acquisition, Supervision. **Yunfeng Yang:** Funding acquisition, Supervision, Writing – original draft.

Declaration of competing interest

The authors declare that they have no known competing financial interests or personal relationships that could have appeared to influence the work reported in this paper.

Acknowledgments

This work was supported by the National Natural Science Foundation of China (grant numbers 41825016, 32161123002, 41877048, & 51938001) and the China National Key Research and Development Program (grant number 2019YFC1806204).

Data availability

DNA representing sequences and OTU tables generated from 16S rRNA genes and ITS are available on GitHub at https://github.com/oneflyer/4-month-microbial-community.git. GeoChip data is available in the NCBI GEO database under project no. GSE190739.

Appendix A. Supplementary data

Supplementary data to this article can be found online at https://doi.org/10.1016/j.scitotenv.2022.157992.

References

Aelion, C.M., Warttinger, U., 2010. Sulfide inhibition of nitrate removal in coastal sediments. Estuar. Coasts 33, 798–803.
Allen, D.E., Dalal, R.C., Rennenberg, H., Meyer, R.L., Reeves, S., Schmidt, S., 2007. Spatial and temporal variation of nitrous oxide and methane flux between subtropical mangrove sediments and the atmosphere. Soil Biol. Biochem. 39, 622–631.
Alongi, D.M., 1988. Bacterial productivity and microbial biomass in tropical mangrove sediments. Microb. Ecol. 15, 59–79.
Alongi, D.M., 2014. Carbon cycling and storage in mangrove forests. Annu. Rev. Mar. Sci. 6, 195–219.
Alongi, D.M., de Carvalho, N.A., Amaral, A.L., Costa, Ad., Trott, L., Tirendi, F., 2012. Uncoupled surface and below-ground soil respiration in mangroves: implications for estimates of dissolved inorganic carbon export. Biogeochemistry 109, 151–162.
Alongi, D.M., Pfitzner, J., Trott, L.A., Tirendi, F., Dixon, P., Klumpp, D.W., 2005. Rapid sediment accumulation and microbial mineralization in forests of the mangrove Kandelia candel in the Jiulongjiang Estuary, China. Estuar. Coast. Shelf Sci. 63, 605–618.
Bai, E., Li, S., Xu, W., Li, W., Dai, W., Jiang, P., 2013. A meta-analysis of experimental warming effects on terrestrial nitrogen pools and dynamics. New Phytol 199, 441–451.
Bernard, R.J., Mortazavi, B., Kleinhuizen, A.A., 2015. Dissimilatory nitrate reduction to ammonium (DNRA) seasonally dominates NO_3^- reduction pathways in an anthropogenically impacted sub-tropical coastal lagoon. Biogeochemistry 125, 47–64.
Braker, G., Schwarz, J., Conrad, R., 2010. Influence of temperature on the composition and activity of denitrifying soil communities. FEMS Microbiol. Ecol. 73, 134–148.
Brunet, R.C., Garcia-Gil, L.J., 1996. Sulfide-induced dissimilatory nitrate reduction to ammonia in anaerobic freshwater sediments. FEMS Microbiol. Ecol. 21, 131–138.
Cao, H., Li, M., Hong, Y., Gu, J.D., 2011. Diversity and abundance of ammonia-oxidizing archaea and bacteria in polluted mangrove sediment. Syst. Appl. Microbiol. 34, 513–523.
Cao, W., Yang, J., Li, Y., Liu, B., Wang, F., Chang, C., 2016. Dissimilatory nitrate reduction to ammonium conserves nitrogen in anthropogenically affected subtropical mangrove sediments in Southeast China. Mar. Pollut. Bull. 110, 155–161.
Chen, L., Tam, N.F.Y., Wang, W., Zhang, Y., Lin, G., 2013. Significant niche overlap between native and exotic sonneratia mangrove species along a continuum of varying inundation periods. Estuar. Coast. Shelf Sci. 117, 22–28.
Craig, H., Antwis, R.E., Cordero, I., Ashworth, D., Robinson, C.H., Osborne, T.Z., et al., 2021. Nitrogen addition alters composition, diversity, and functioning of microbial communities in mangrove soils: an incubation experiment. Soil Biol. Biochem. 153, 108076.
Edgar, R.C., Haas, B.J., Clemente, J.C., Quince, C., Knight, R., 2011. UCHIME improves sensitivity and speed of chimera detection. Bioinformatics 27, 2194–2200.
Enebe, M.C., Babalola, O.O., 2021. The influence of soil fertilization on the distribution and diversity of phosphorus cycling genes and microbes community of maize rhizosphere using shotgun metagenomics. Genes (Basel) 12, 1022.
Friedlingstein, P., Jones, M.W., O'Sullivan, M., Andrew, R.M., Bakker, D.C.E., Hauck, J., et al., 2022. Global carbon budget 2021. Earth Syst. Sci. Data 14, 1917–2005.
Gao, G.-F., Li, P.-F., Zhong, J.-X., Shen, Z.-J., Chen, J., Li, Y.-T., et al., 2019. Spartina alterniflora invasion alters soil bacterial communities and enhances soil N_2O emissions by stimulating soil denitrification in mangrove wetland. Sci. Total Environ. 653, 231–240.
Grant, R.F., Pattey, E., 2008. Temperature sensitivity of N_2O emissions from fertilized agricultural soils: mathematical modeling in ecosys. Glob. Biogeochem. Cycl. 22, 1754–1755.
Gruber, N., Galloway, J.N., 2008. An earth-system perspective of the global nitrogen cycle. Nature 451, 293–296.

IPCC, 2014. Climate change 2014: synthesis report. In: Team, Core Writing, Pachauri, R.K., Meyer, L.A. (Eds.), Contribution of working groups I, II and III to the Fifth Assessment Report of the the Intergovernmental Panel on Climate Change. IPCC, Geneva, Switzerland, pp. 151–152.
Jia, D., Qi, F., Xu, X., Feng, J., Wu, H., Guo, J., et al., 2016. Co-regulations of Spartina alterniflora invasion and exogenous nitrogen loading on soil N_2O efflux in subtropical mangrove mesocosms. PLoS ONE 11, e0146199.
Kong, Y., 2011. Btrim: a fast, lightweight adapter and quality trimming program for next-generation sequencing technologies. Genomics 98, 152–153.
Koops, H.-P., Pommerening-Röser, A., 2001. Distribution and ecophysiology of the nitrifying bacteria emphasizing cultured species. FEMS Microbiol. Ecol. 37, 1–9.
Koyama, A., Wallenstein, M.D., Simpson, R.T., Moore, J.C., 2014. Soil bacterial community composition altered by increased nutrient availability in Arctic tundra soils. Front. Microbiol. 5, 516.
Kristensen, E., Bouillon, S., Dittmar, T., Marchand, C., 2008. Organic carbon dynamics in mangrove ecosystems: a review. Aquat. Bot. 89, 201–219.
Lei, J., Guo, X., Zeng, Y., Zhou, J., Gao, Q., Yang, Y., 2021. Temporal changes in global soil respiration since 1987. Nat. Commun. 12, 403.
Lewis, D.B., Brown, J.A., Jimenez, K.L., 2014. Effects of flooding and warming on soil organic matter mineralization in Avicennia germinans mangrove forests and Juncus roemerianus salt marshes. Estuar. Coast. Shelf Sci. 139, 11–19.
Li, M., Fang, A., Yu, X., Zhang, K., He, Z., Wang, C., et al., 2021. Microbially-driven sulfur cycling microbial communities in different mangrove sediments. Chemosphere 273, 128597.
Liu, Z., Zhang, C., Wei, Q., Zhang, S., Quan, Z., Li, M., 2020. Temperature and salinity drive comammox community composition in mangrove ecosystems across southeastern China. Sci. Total Environ. 742, 140456.
Livesley, S.J., Andrusiak, S.M., 2012. Temperate mangrove and salt marsh sediments are a small methane and nitrous oxide source but important carbon store. Estuar. Coast. Shelf Sci. 97, 19–27.
Lovelock, C.E., Feller, I.C., Reef, R., Hickey, S., Ball, M.C., 2017. Mangrove dieback during fluctuating sea levels. Sci. Rep. 7, 1680.
Luo, C., Rodriguez-R, L.M., Johnston, E.R., Wu, L., Cheng, L., Xue, K., et al., 2014. Soil microbial community responses to a decade of warming as revealed by comparative metagenomics. Appl. Environ. Microbiol. 80, 1777–1786.
Luo, L., Meng, H., Wu, R.-n., Gu, J.-D., 2017. Impact of nitrogen pollution/deposition on extracellular enzyme activity, microbial abundance and carbon storage in coastal mangrove sediment. Chemosphere 177, 275–283.
Ma, X., Zhang, Q., Zheng, M., Gao, Y., Yuan, T., Hale, L., et al., 2019. Microbial functional traits are sensitive indicators of mild disturbance by lamb grazing. ISME J. 13, 1370–1373.
Magoč, T., Salzberg, S.L., 2011. FLASH: fast length adjustment of short reads to improve genome assemblies. Bioinformatics 27, 2957–2963.
Muñoz-Hincapié, M., Morell, J.M., Corredor, J.E., 2002. Increase of nitrous oxide flux to the atmosphere upon nitrogen addition to red mangroves sediments. Mar. Pollut. Bull. 44, 992–996.
Murray Nicholas, J., Worthington Thomas, A., Bunting, P., Duce, S., Hagger, V., Lovelock Catherine, E., et al., 2022. High-resolution mapping of losses and gains of Earth's tidal wetlands. Science 376, 744–749.
Page, A., Miller, R., Keeney, D., 1982. Methods of soil analysis, part 2. Chemical and Microbiological Properties. 2, pp. 643–698.
Prosser, J.I., Nicol, G.W., 2012. Archaeal and bacterial ammonia-oxidisers in soil: the quest for niche specialisation and differentiation. Trends Microbiol. 20, 523–531.
Rao, N.N., Gomez-Garcia, M.R., Kornberg, A., 2009. Inorganic polyphosphate: essential for growth and survival. Annu. Rev. Biochem. 78, 605–647.
Reef, R., Feller, I.C., Lovelock, C.E., 2010. Nutrition of mangroves. Tree Physiol. 30, 1148–1160.
Reis, C.R.G., Nardoto, G.B., Oliveira, R.S., 2017. Global overview on nitrogen dynamics in mangroves and consequences of increasing nitrogen availability for these systems. Plant Soil 410, 1–19.
Sarker, S.K., Matthiopoulos, J., Mitchell, S.N., Ahmed, Z.U., Mamun, M.B.A., Reeve, R., 2019. 1980s 2010s: the world's largest mangrove ecosystem is becoming homogeneous. Biol. Conserv. 236, 79–91.
Schröter, D., Wolters, V., De Ruiter, P.C., 2003. C and N mineralisation in the decomposer food webs of a european forest transect. Oikos 102, 294–308.
Shiau, Y.-J., Dham, V., Tian, G., Chiu, C.-Y., 2016. Factors influencing removal of sewage nitrogen through denitrification in mangrove soils. Wetlands 36, 621–630.
Snedaker, J., Snedaker, S., 1984. The Mangrove Ecosystem: Research Methods. United Nations Educational, Scientific and Cultural Organization.
Spalding, M., Leal, M., 2021. The state of the world's mangroves 2021. Global Mangrove Alliance.
Stegen, J.C., Lin, X., Konopka, A.E., Fredrickson, J.K., 2012. Stochastic and deterministic assembly processes in subsurface microbial communities. ISME J. 6, 1653–1664.
Thakur, N.K., Singh, R., Ojha, A., 2021. Dynamical study of harmful algal bloom in sundarban mangrove wetland with spatial interaction and competing effects. Modeling Earth Systems and Environment, pp. 1–23.
Thauer, R.K., Jungermann, K., Decker, K., 1977. Energy Conservation in Chemotrophic Anaerobic Bacteria. 41. American Society for Microbiology, pp. 100–180.
Toso, D.B., Henstra, A.M., Gunsalus, R.P., Zhou, Z.H., 2011. Structural, mass and elemental analyses of storage granules in methanogenic archaeal cells. Environ. Microbiol. 13, 2587–2599.
Wang, C., Liu, D., Bai, E., 2018. Decreasing soil microbial diversity is associated with decreasing microbial biomass under nitrogen addition. Soil Biol. Biochem. 120, 126–133.
Wang, F., Sanders, C.J., Santos, I.R., Tang, J., Schuerch, M., Kirwan, M.L., et al., 2021. Global blue carbon accumulation in tidal wetlands increases with climate change. Natl. Sci. Rev. 8, nwaa296.
Wang, Q., Garrity, G.M., Tiedje, J.M., Cole, J.R., 2007. Naive bayesian classifier for rapid assignment of rRNA sequences into the new bacterial taxonomy. Appl. Environ. Microbiol. 73, 5261–5267.
Wu, H., Peng, R., Yang, Y., He, L., Wang, W., Zheng, T., et al., 2014. Mariculture pond influence on mangrove areas in South China: significantly larger nitrogen and phosphorus loadings from sediment wash-out than from tidal water exchange. Aquaculture 426–427, 204–212.
Wu, L., Yang, Y., Chen, S., Jason Shi, Z., Zhao, M., Zhu, Z., et al., 2017. Microbial functional trait of rRNA operon copy numbers increases with organic levels in anaerobic digesters. ISME J. 11, 2874–2878.
Xue, K., Yuan, M.M., Shi, J.Z., Qin, Y., Deng, Y., Cheng, L., et al., 2016. Tundra soil carbon is vulnerable to rapid microbial decomposition under climate warming. Nat. Clim. Chang. 6, 595–600.
Ya, T., Du, S., Li, Z., Liu, S., Zhu, M., Liu, X., et al., 2021. Successional dynamics of molecular ecological network of anammox microbial communities under elevated salinity. Water Res. 188, 116540.
Yang, W.H., Silver, W.L., 2016. Gross nitrous oxide production drives net nitrous oxide fluxes across a salt marsh landscape. Glob. Chang. Biol. 22, 2228–2237.
Yang, Y., Gao, Y., Wang, S., Xu, D., Yu, H., Wu, L., et al., 2014. The microbial gene diversity along an elevation gradient of the tibetan grassland. ISME J 8, 430–440.
Zhang, J., Gao, Q., Zhang, Q., Wang, T., Yue, H., Wu, L., et al., 2017. Bacteriophage–prokaryote dynamics and interaction within anaerobic digestion processes across time and space. Microbiome 5, 57.
Zhang, Q., Zhou, J., Li, X., Zheng, Y., Xie, L., Yang, Z., et al., 2022. Contrasting effects of warming and N deposition on soil microbial functional genes in a subtropical forest. Geoderma 408.
Zhou, J., Xue, K., Xie, J., Deng, Y., Wu, L., Cheng, X., et al., 2011. Microbial mediation of carbon-cycle feedbacks to climate warming. Nat. Clim. Chang. 2, 106–110.